PERGAMON

International Journal of Impact Engineering 23 (1999) 639–649

INTERNATIONAL JOURNAL OF IMPACT ENGINEERING

www.elsevier.com/locate/ijimpeng

STATISTICAL ANALYSIS OF NRL 1964-1969 HYPERVELOCITY ROD-PLATE IMPACT DATA AND COMPARISON TO RECENT DATA

P.E. NEBOLSINE*, N.D. HUMER*, N.F. HARMON*, and J.R. BAKER**

*Physical Sciences Inc., 20 New England Business Center, Andover, MA 01810-1077, USA;
**U.S. Naval Research Laboratory, Washington, DC 20375, USA

Summary — The previously reported Naval Research Laboratory hypervelocity rod-plate impact database was studied to derive the statistical variation that could be assigned to measurements of rod erosion for various impact conditions and impacting materials. The database covers impacts of 3.175 mm diameter rods having diameter-to-length ratios of 10 at velocities between 2.6 and 6.1 km/s upon targets whose thickness varied from 0.0355 to 6.5 rod diameters. Seven different projectile materials and 10 different target materials as well as alloys of aluminum and steel were tested. Of the 275 individual impacts reported, 157 were selected for statistical analysis. It was found that all of the data were normally distributed with a mean of 0.966 and standard deviation of 7.6% of the mean when the individual experimental measurements of rod erosion were normalized to predicted values calculated for the same impact conditions using the semi-empirical equation reported by Baker. Using this normalization, recent data from a multiple plate impact experiment was found to lie well within the uncertainty band. Subsets of the data are discussed.

INTRODUCTION

In engineering studies on the lethal effectiveness of hypervelocity rod attack on complex structures the damage created by the rod is defined in terms of its ability to penetrate into or through its target. For many targets this penetrating ability is conveniently stated in terms of the rod shortening, i.e., erosion, experienced during the penetration and perforation processes. In order to perform meaningful systems engineering weapons effectiveness studies a rapid method of calculating the erosion under different engagement and impact conditions is required along with the uncertainties in the calculated results. Such a rapid computational technique can be applied to a wide variety of engagements and knowledge of the uncertainties in the results are necessary to define quantitatively the statistical characteristics of the weaponry under study. The speed requirement obviates the use of detailed numerical calculations, e.g., hydrocodes, and argues for the use of an analytic calculation based upon the results of both detailed computations and experimental data. This was the approach undertaken at the Naval Research Laboratory (NRL) using a large experimental data base generated over several years [1-3] and the results of two dimensional hydrodynamic calculations simulating the impact processes for certain impact conditions. A fortuitous consequence of the large data base available is that many repeat conditions and a range of impact conditions are available from the same experimental apparatus and analysts. This allows a statistical analysis of the data which is the purpose of this paper.

0734-743X/99/$ - see front matter
PII: S0734-743X(99)00110-4

BACKGROUND

Baker [3,4] reported a simple, semi-empirical equation (henceforth called the Baker equation) for rod loss , $\Delta\ell$, as a function of the rod impact parameters for hypervelocity perforation of a plate of the same material. This equation is:

$$\frac{\Delta\ell}{d} = \frac{t}{d} + \frac{\Delta t}{d} + \frac{v\tau}{d}\left\{1 - \exp\left[-\left(\frac{\Delta\ell/d + t/d + \Delta t/d}{f\, v\, \tau/d}\right)\right]\right\} \tag{1}$$

where all lengths have been normalized by the rod diameter, d. t is the target thickness, v is the impact velocity, and f, τ, and $\Delta t/d$ are empirical constants. Note that Eqn. (1) must be solved iteratively since the unknown parameter $\Delta\ell/d$ appears on both sides of the equation.

The first term in Eqn. (1), t/d, is simply the length loss commonly associated with steady-state hydrodynamic erosion. The second term, $\Delta t/d$, is a small additional loss due to a non-steady-state process that is possibly associated with the initial shock phase of the impact process. For most cases of practical interest ($t/d > 0.05$), this term can be taken as a constant; however, as noted below, this is not strictly true. The third term, involving $v\tau/d$, is the primary non-steady state loss associated with the final breakout phase of the perforation process. The value of $v\tau/d$ can be computed from the equation:

$$\frac{v\tau}{d} = \frac{1.98\ v}{\sqrt{[c^2 - (u_s - v/2)^2]}} \tag{2}$$

where c is the sound speed in the shocked rod material, and u_s is the shock velocity. These quantities can be obtained using either published equation-of-state data or coefficients for the approximation that the shock velocity is a linear function of the particle velocity.

It should be noted that for thick target plates ($t/d > 2$) the rod loss approaches a linear dependence on t/d given by

$$\frac{\Delta\ell}{d} = \frac{t}{d} + \frac{\Delta t}{d} + \frac{v\tau}{d}$$

with constant transient erosion terms of $\Delta t/d + v\tau/d$. For very thin target plates ($t/d < 0.1$), the term $\Delta t/d$ in Eqn. (1) should be replaced by the expression $(\Delta t/d)\,[1 - \exp(-\xi t/d)]$ so that the rod loss approaches zero as t/d approaches zero. The effect of this modification is however negligible for $t/d > 0.05$.

Equation (1) was generated by adding the empirical constants cited to a theoretical model describing the impact process such that the resultant equation fit both the computer generated results for hole depth and the experimental data for rod erosion in the case of aluminum on aluminum impacts (Baker [3]).

For an impact configuration in which the projectile and target plate are of different materials, the rod loss can still be computed using a modification of Eqn. (1). By analogy with the theory of steady state, incompressible hydrodynamic penetration modeling which predicts that for unlike fluids, the penetration varies as the square root of the density ratio of the two fluids, so too did Baker [3] find the normalized rod erosion depend on the rod and target material densities, i.e.,

$$\left(\frac{\Delta\ell}{d}\right)_{1\to 2} = \sqrt{\left(\frac{\rho_2}{\rho_1}\right)}\left(\frac{\Delta\ell}{d}\right)_{1\to 1} \tag{3}$$

where 1→2 signifies rod material of density, ρ_1, impacting target material, ρ_2. This paper will examine the NRL experimental database in the light of the Baker equation in order to generate the statistical parameters associated with rod loss predictions made with the equation.

The main focus of the NRL experiments was centered on using 2024-T86 aluminum rods 0.3175 mm (1/8 in.) in diameter with a length to diameter ratio (l/d) of ~10, impacting 2024-T3 plates at 90 deg (normal impact) and a nominal 4.6 km/s impact velocity. This data was used in determining the dependence of rod loss on impact conditions and target thickness. In addition, a substantial amount of data was generated to study the effect of changing the various impact conditions, e.g., target and rod material, rod diameter, impact velocity and impact angle. Table 1 lists the various combinations and the number of data points attempted. Of the of the 275 individual impacts listed in this table, 54% were aluminum rod-aluminum plate impacts , about 18% were steel rod-steel plate impacts with the remaining 36% unevenly distributed among seven different projectile materials and eight different target materials.

ANALYSIS

This analysis will examine the aluminum rod-aluminum plate impacts in two steps: 1) examine the rod erosion dependence on target thickness for the experimental data taken at impact velocities of (4.65 ± 0.233)km/s, and 2) expand the analysis to data taken at other impact velocities. This will be followed by a discussion of the distribution of this data about its mean. The analysis will then be expanded to include the other rod-target material pairs though application of the square root of the density ratio scaling of Eqn. (3).

For the analysis highly yawed rods (greater than 10 deg), oblique impacts, impact velocities less than 2.3 km/s, and experimental points for which the pre-impact rod length were unspecified were excluded. In addition those experiments using tool steel rods were excluded since there was experimental evidence that rod loss continued after plate perforation rendering the quoted values suspect [2]. These exclusions left 165 impacts for analysis. For the aluminum on aluminum impacts, this left 79 experimental data points spanning the velocity range from 2.3 to 6.1 km/s while the target thickness varied from 0.035 to 6.5 rod diameters. Of the 79, 9 were 2024-T86 rods and 1100 F targets, 7 were 2024-T3 rods and 2024-T3 targets the rest being 2024-T86 rods and 2024-T3 targets. Forty-seven of these data points are for impacts in the (4.65 ± 0.233) km/s range.

Nearly Constant Velocity Aluminum Rod-Aluminum Plate Impacts

Figure 1 shows the measured erosion for a the subset of the aluminum on aluminum data taken at impacts in the nearly constant (4.65 ± 0.233) km/s range plotted versus target thickness each being normalized to the rod diameter, a convention that will be followed throughout this paper. The sloping line in the figure is the prediction from Eqn. (1) of the erosion for the indicated thickness at an impact velocity of 4.65 km/s. This curve appears to give a good fit to the data. The triangles centered near the scaled erosion of 1.0 mark are the experimental erosion normalized to that predicted by the Baker equation for the same impact conditions. The large amount of scatter for thickness less than about 0.5 rod diameters is the result of the small erosion and the appearance of

Table 1. Summary of NRL rod impact conditions

Projectile Material	Plate Material	t/d	Impact Velocity (km/s)	Shots	Plate Angle
2024 Aluminum	2024 Aluminum	0.16 - 5.5	4.6, 6.1	83	90 deg
↓	↓	1.0	0.5 - 6.3	37	90 deg
		0.25 - 2.0	4.1 - 4.6	18	10 - 60 deg
	1100F Aluminum	0.03 - 2.0	4.4 - 4.7	11	90 deg
	4340 Steel	0.4 - 2.0	4.6	9	
	Copper	0.5 - 2.0	4.6	8	
	Lead	1.0 - 1.5	4.6	5	
	Zinc	1.0 - 2.0	4.6	3	
↓	Uranium	0.25, 1.0	4.6	3	
	1020 Steel	0.9	1.3	2	
	Cold Rolled Steel	1.0	4.5	1	
	6061 Aluminum	0.1	4.6	1	
	Titanium	0.5	4.7	1	
	Magnesium	3.0	4.1	1	
	Phenolic Refrasil	2.2	4.6	1	
4340 Steel	4340 Steel	1.0	1.3 - 5.9	17	
↓	↓	0.16 - 2.0	4.5	4	↓
		0.25, 1.0	4.6	3	10 - 20 deg
↓	2024 Aluminum	0.25 - 8.0	4.0 - 4.5	6	90 deg
	Cold Rolled Steel	0.22	4.7	3	10 - 20 deg
	Uranium	1.0	4.6	1	90 deg
	Magnesium	3.2, 3.5	5.3 - 5.6	2	
Tool Steel	2024 Aluminum	0.25 - 2.0	4.2 - 4.6	15	
Nickel	Nickel	0.25 - 1.0	4.0	5	
↓	2024 Aluminum	1.0	4.4	2	
	Copper	0.75 - 2.0	4.2 - 4.4	6	
Uranium	Uranium	1.0	1.4 - 3.7	5	
	2024 Aluminum	0.75 - 3.5	3.1, 3.8	4	
↓	Uranium	0.3 - 1.5	3.1	3	
	Titanium	1.1 - 2.4	3.1	3	
Tungsten	Tungsten	1.0	4.0	1	
↓	2024 Aluminum	0.5 - 1.0	3.9 - 4.4	3	
Titanium	Titanium	0.5 - 1.0	4.5	5	
↓	↓	0.23	3.2, 4.0		
	Uranium	0.5 - 1.0	4.6	3	↓

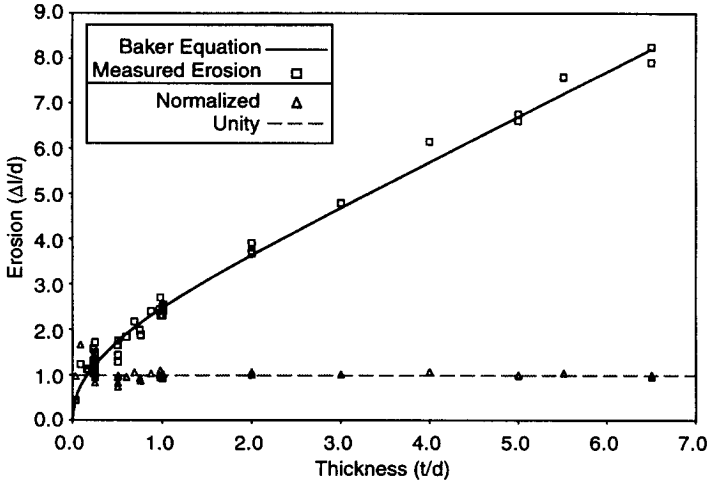

Fig. 1. NRL Al on Al data (4.412 < v < 4.883 km/s).

the front of the rods in the flash x-ray images. The rod tip is jagged rather than smooth as in the case for thick target impacts. Both of these effects lead to the increased data scatter [1] for the thin plate data. As is clear from the figure for aluminum rods impacting aluminum plates, there are target thicknesses for which several data points are available. Table 2 lists these target thickness ratios (A) along with the average of the measured erosion, (B), the root mean square (rms) deviation about the average (C), the fractional deviation (D) (the rms value ÷ Δℓ/d (column C ÷ column B)), the erosion calculated using the Baker equation (E), the ratio of the averages of the measured erosions to calculated (Baker) erosion (F) (equivalent to B ÷ E), and the rms deviation of these ratios (G), along with its fractional deviation

Table 2. Comparison of measured to calculated erosion for aluminum rods impacting aluminum plates.

A	*B*	*C*	*D*	*E*	*F*	*G*	*H*
Target thickness ratio (t/d)	*Average erosion* $\left(\frac{\Delta\ell}{d}\right)$	*rms deviation* $\left(\frac{\Delta\ell}{d}\right)$	*Fractional deviation*	*Cacluated erosion* $\left(\frac{\Delta\ell}{d}\right)$	*Measured ÷ calculated erosion*	*rms deviation* $\left(\frac{\Delta\ell}{d}\right)$	*Fractional deviation*
0.233	1.379	0.139	0.10	1.200	1.150	0.114	0.10
0.250	1.360	0.215	0.16	1.238	1.099	0.173	0.16
0.50	1.536	0.180	0.12	1.741	0.880	0.102	0.12
1.0	2.442	0.131	0.054	2.477	0.987	0.054	0.053
2.0	3.743	0.084	0.02	3.638	1.028	0.023	0.02
5.0	6.686			6.700	1.000		
5.5	7.585			7.200	1.050		
6.5	8.080			8.200	0.984		

(H). All dimensions are normalized to the rod diameter. Although the Baker equation was not fit at these points, the agreement between experiment and calculation is good. Column F for the measured divided by the calculated erosion gives a measure of the agreement between the two. In general, the agreement is quite good particularly for the thicker targets although there are too few

data points available for meaningful rms deviation calculations at the three largest thicknesses. The fractional deviation in this ratio is the fractional deviation in the experimental data as shown by comparing the fourth and last columns in the table. The use of this ratio affords a means of comparing all of the data and generating a standard deviation that applies to the entire data set.

For the data shown in Fig. 1 by the triangle centered near the scaled erosion of 1.0 line, the measured/calculated erosion has an average value of 1.037 with an rms deviation of 0.15. Thus the Baker equation, on average, under-predicts the experimental results but not to a significant degree. Excluding the experimental data for plate thickness less than 0.6 rod diameters the average measured/calculated erosion for the remaining 31 data points is 1.003 with a rms deviation of 0.05. This success of the Baker equation in predicting the experimental result is encouraging since it represents a semi-empirical rather than an empirical fit to the data.

All Aluminum Rod-Aluminum Plate Impacts

Figure 2 shows the measured normalized erosion scaled by Eqn. (1) to 4.65 km/s for the full velocity range of the NRL aluminum on aluminum data plotted versus the target thickness rate. Note that the additional data are for target thicknesses of 3.0 rod diameters and less. As expected for the range of impact conditions represented, the apparent data scatter is increased. As in Fig. 1 the points marked with triangles near the horizontal line at a scaled erosion of 1.0 on the plot are the experimental erosion normalized to the Baker equation result at the same experimental condition. In this case the average of the measured/calculated erosion is 1.027 with an rms deviation of 0.13. Thus, even with this expansion in experimental conditions beyond those for which the Baker equation was intended, it still predicts, on average, the experimental erosion. Excluding target thicknesses less than 0.6 rod diameters yields an average measured/calculated erosion of 1.011 with an rms deviation of 0.06, a striking agreement of calculation with measurement.

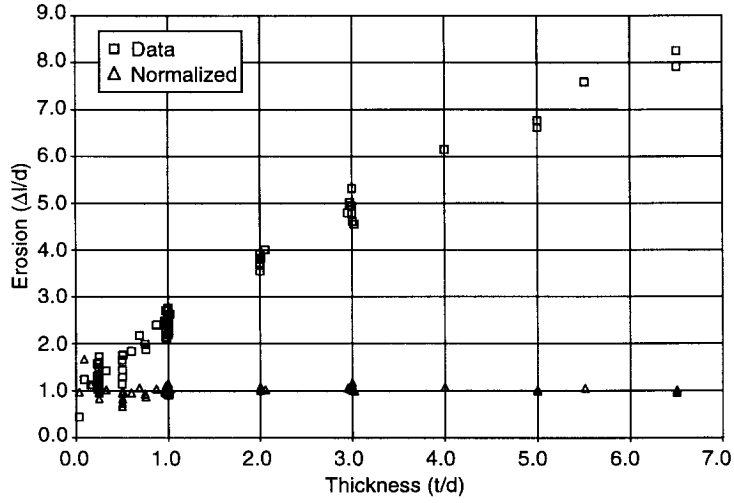

Fig. 2. Velocity scaled NRL Al on Al data (all impact velocities).

The experimental data for the thinner targets represents a different class of data from that for the thicker targets as a result of the difficulty in making the measurements. For the 24 data points available, for normalized target thickness less than 0.6 rod diameters the average measured/calculated erosion is 1.06 with an rms deviation of 0.22. Thus, on average, the Baker equation is in good agreement with the experimental data even though the data scatter is large.

Distributions

Figure 3 shows a more graphic illustration of this scatter. In this figure, the experimental data normalized to the Baker equation result for the same experimental conditions and the experimental

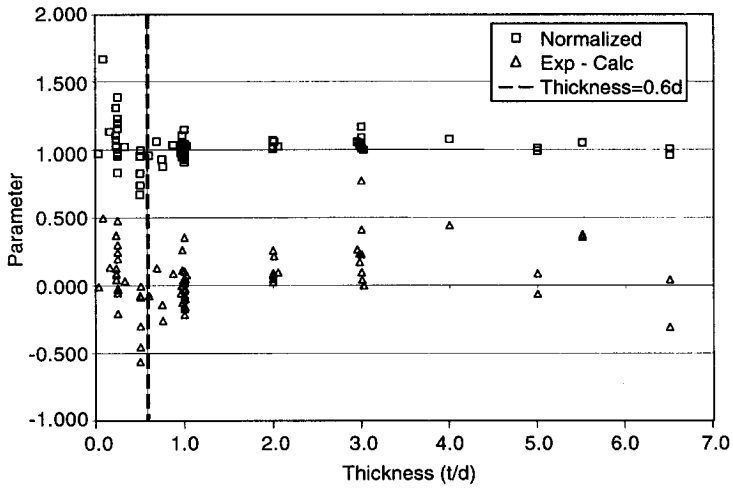

Fig. 3. Scaled NRL Al on Al data.

data minus the calculated result (exp-cal) are displayed as a function of thickness. The exp-calc points show a tendency for the calculations to underestimate the experimental data at thicknesses greater than two rod diameters however the fractional deviation is not large as is evident by the scatter in the points of the normalized data. At the lesser thicknesses the large scatter in the deviations is almost evenly distributed and the fractional deviations are large as is reflected in the scatter in the normalized points. Considering the points to the right and left of the vertical line at just under 0.6 rod diameters illustrates the makeup of the data whose averages were presented previously.

Figure 4 shows the distribution of the normalized data and compares it to two normal distributions having the same mean but different rms deviations. The distribution of the data is slightly skew, by about 3% toward higher values than the average as expected from Fig. 3. This distribution is symmetric about its mean. Comparing Fig. 4 with Fig. 3 shows that the outliers are mainly from the thinner plate data where the scatter is greater. The Normal 1 curve is a normal distribution having the same mean and rms deviation as the data. This curve appears to overestimate the rms deviation exhibited by the data in this plot. The Normal 2 curve is a normal distribution having the same mean as the data but with an rms deviation calculated from the average amplitude of the data at its peak, 5.8, yielding an rms deviation of 0.069 as shown on the plot. This distribution gives a better fit at the peak but increase the number of outliers. Figure 5 shows the cumulative distributions derived from the plots of Fig. 4. The very steep rise in the data near its average is not mirrored in either of the normal distributions. The Cumulative 1 curve, with same mean and rms deviation as the data, doesn't match the data. On the other hand, the Cumulative 2 curve, with the same mean and rms deviation as derived from the data peak, is a good match to the data except at its extremes. In the case of the former distribution 16% of the data points lie outside the rms deviation while for the latter distribution 36% do.

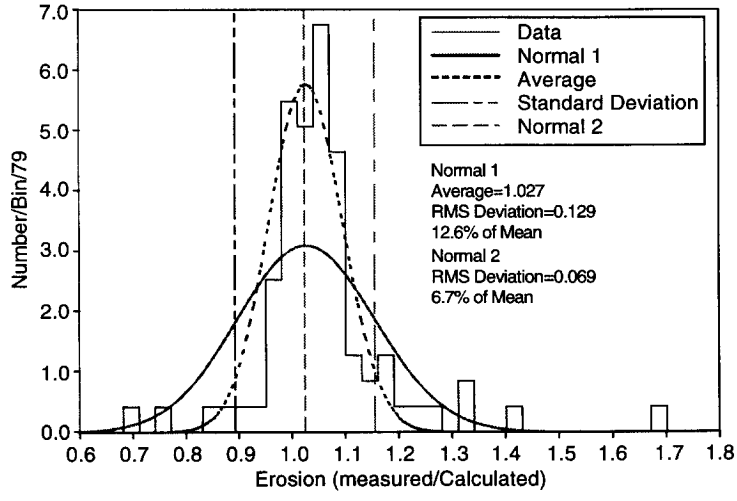

Fig. 4. Scaled NRL Al data histogram distributions.

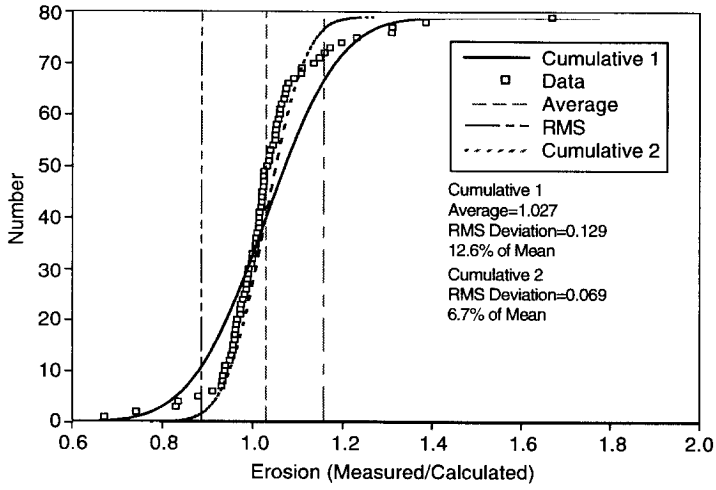

Fig. 5. Scaled NRL Al data, cumulative distribution.

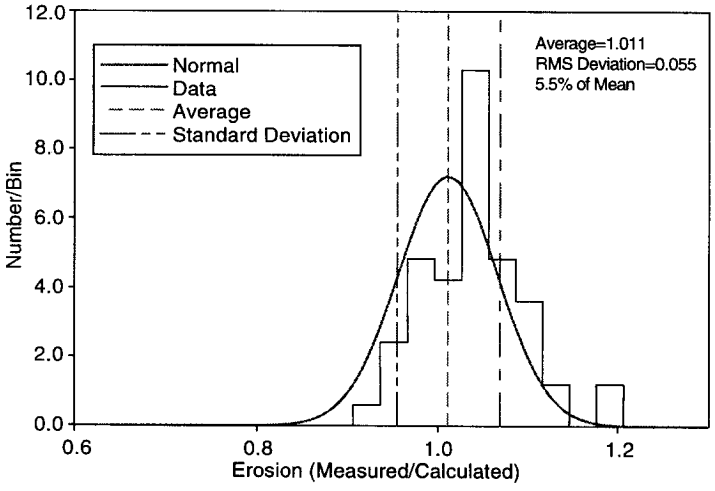

Fig. 6. Scaled NRL Al data histogram distributions (t/d > 0.6).

Figure 6 shows the distribution resulting from excluding the data for plate thickness less than 0.6 rod diameters compared with a normal distribution having the same mean and rms deviation as the data. The distribution is a good match to the data. As expected, the distribution of the data is much narrower with fewer outliers. It maintains the slight skewness and concentration of data near and just above the average. Figure 7 shows the cumulative distribution of this data and illustrates both the good fit of the normal distribution and the slight peakiness of the data near its upper rms deviation. These plots show that the NRL aluminum data normalized to the value calculated by the Baker equation is well represented as a normal distribution.

Density Scaling

Extending the analysis to the entire database includes unlike rod and target material impacts. To provide for comparison of data taken at different conditions, the Baker equation provides a common condition of v = 4.65 km/s and t/d = 1. Then all the data for each projectile and target material pair has been averaged. Scaling for density is accomplished by applying Eqn. (3), the square root of density ratio scaling (hydrodynamic limit scaling), to all of the rod projectile-target combinations. Figure 8 is a plot for each projectile and target material combination of the scaled averaged data versus the square root of the ratio of target density to projectile density. The solid line on this plot is the Baker prediction for the scaled erosion given its value for like material impacts. Note that for like material impacts the mean scaled erosion is nearly material independent. This scaling is expected to apply to the steady-state erosion associated with penetration [5], but not necessarily to the non-steady-state part of the process. Figure 8 indicates that it applies to both processes. Figure 9 shows the scaled measured erosion versus target thickness for all of the data scaled through the Baker equation to an aluminum on aluminum impact at a velocity of 4.65 km/s to examine only t/d dependence. This scaling is accomplished by multiplying the experimental data by the Baker

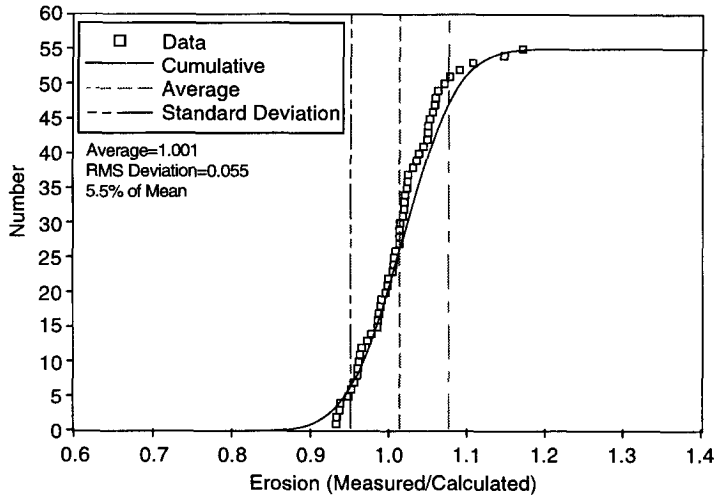

Fig. 7. Scaled NRL Al data, cumulative distribution (t/d > 0.6).

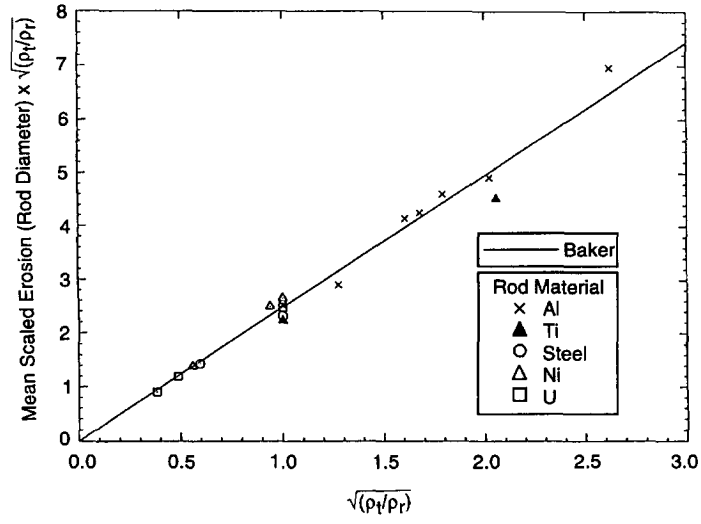

Fig. 8. Scaled mean erosion versus square root of target/rod density ratio (Baker 1969 data).

equation predicted erosion for an aluminum rod impacting an aluminum plate at a velocity of 4.65 km/s and the square root of the density ratio and dividing this product by the Baker equation prediction for impact conditions corresponding to the experimental data. The solid line on this plot is the Baker equation prediction for these conditions. Comparing Fig. 9 with Fig. 2 shows that the additional 86 data points tend to increase the scatter in the data. Figure 10 shows the distributions for the experimental erosion minus the calculated erosion and the measured/calculated erosion for the experimental data shown in Fig. 9 excluding the aluminum on aluminum data for thicknesses less than 0.6 rod diameters. Here the normalized data and the experimental minus the calculated erosion are plotted versus a number that identifies the rod-plate material combinations. Only the rod material is indicated in the figure. The preponderance of aluminum rods among the 141 points in the data set is clear from this figure. The left portion of this plot, the experimental data minus the calculated value, show that for the aluminum and nickel rods the calculated values tend to underestimate the experimental results more often than not while for the steel and titanium rods the opposite seems to be the case. The normalized erosion shown on the right side of the plot has a mean value of 0.996 with an rms deviation of 0.076, 7.6% of the mean. The points near the 140 marker show a tendency for the calculated values to always overestimate the experimental results. That is a result of the observation that the titanium rods used in those experiments were always eroded less than the other rod materials under the same experimental conditions. Figure 11 shows the cumulative distribution of the data and compares it to a normal distribution having the same mean and rms deviation. Unlike the aluminum data alone shown in Fig. 4, this expanded data set follows fairly closely the normal cumulative distribution much as the subset of aluminum on aluminum data shown in Fig. 6. Once again this close agreement suggests that the data conforms to a normal distribution.

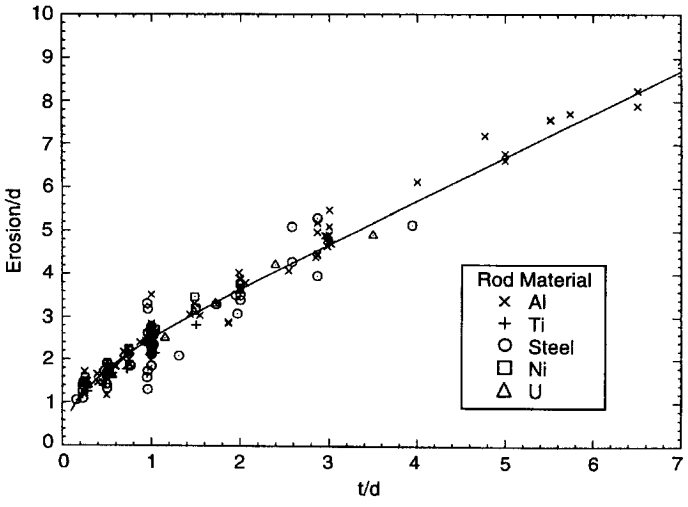

Fig. 9. Normalized NRL rod erosion data for Al, Ti, Fe, Ni, and U rods (1969 data: Baker data, scaled to Al → Al at v = 4.65 km/s).

Recent Experimental Data

Figure 11 also includes recent experimental data from a multi-plate experiment performed in 1996. In that experiment a tungsten-nickel-cobalt alloy rod of 0.42 cm diameter and 5.9 cm length traveling at 3.37 km/s impacted a stack of 0.635 cm (¼ in, t/d = 1.5) thick steel plates separated by approximately 5 cm. The angle of attack was less than 2 deg. Seven plates were perforated and a very modest amount of pitting occurred on the eighth plate. The rod was totally consumed. The Δ on the plot labeled UAH Data, (arbitrarily

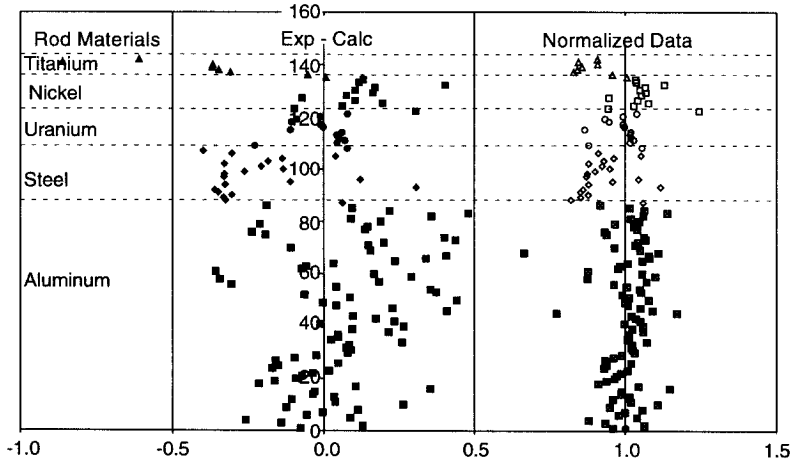

Fig. 10. Scaled NRL data, distributions versus rod material.

vertically positioned), is the experimental data normalized to its Baker equation prediction assuming that perforation of the seventh plate occurred by the rod remnant being above the ballistic limit for that plate. The erosion was calculated for each plate individually and then summed to obtain the final result as suggested in Baker 1987. The agreement with the 30 year old NRL results is striking. We have also examined by what factor the erosion would need to be enhanced or diminished in order to have a total of six or eight plates be penetrated. Those points are also shown in Fig. 11.

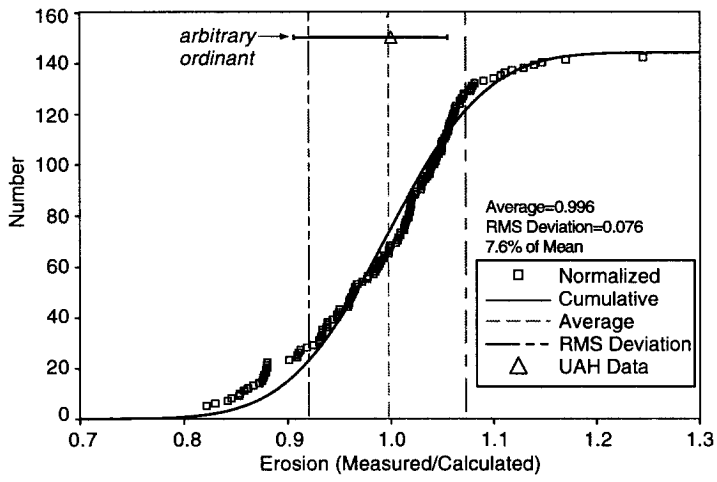

Fig. 11. Scaled NRL data, cumulative distribution.

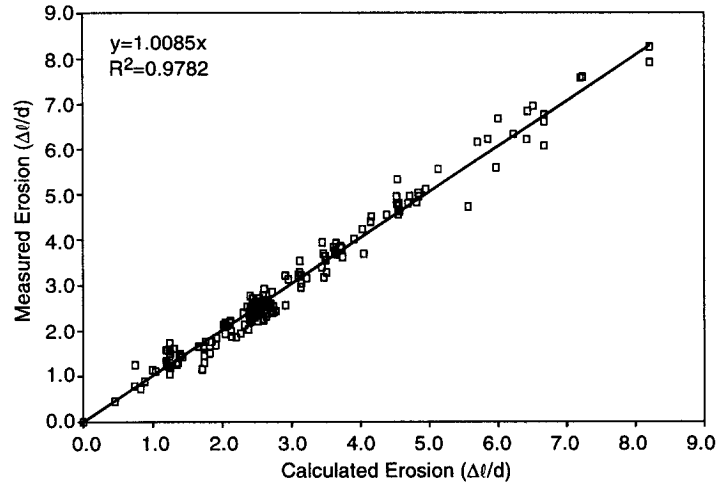

Fig. 12. NRL data, experiment-theory comparison.

Discussion

The preceding analysis has shown not only that the Baker equation is an excellent fit to all of the NRL experimental data but also that the data is distributed approximately normally about the mean with small standard deviation, 7.6% of the mean. Thus one more measurement within the bounds of the data set when normalized with its Baker equation prediction has a 68% chance of lying within the range 0.92 to 1.072. Figure 12 shows the comparison between the experimental and calculated erosion in a slightly different form. Here the calculated erosion is plotted versus the measured erosion for all of the NRL data considered here. The straight line in this plot is a least squares fit to the points shown assuming that the calculated erosion is the independent variable and that the line passes through the origin. This line might prove a convenient "bench mark" for new computations aimed at describing more complex impact conditions.

Acknowledgment—The data for the 5.9 cm tungsten alloy rod impact was provided by the Aerophysics Research Center, University of Alabama in Huntsville.

REFERENCES

1. J.J. Condon, "Rod Lethality Studies," NRL Report ALT-TR-65-18, Naval Research Laboratory, Washington, D.C., March 1965.
2. J. J. Condon and J.R. Baker, "Annual Technical Progress Report on Rod Lethality Studies," NRL Memorandum Report 18092, Naval Research Laboratory, Washington, D.C., September 1967.
3. J.R. Baker, "Rod Lethality Studies," NRL Report 6920, Naval Research Laboratory, Washington, D.C., July 1969.
4. J.R. Baker and A. Williams, "Hypervelocity penetration of plate targets by rod and rod-like projectiles," *Int. J. Impact Engr.* **Vol. 5**, pp.101-110, 1987.
5. Zukas J.A., HIGH VELOCITY IMPACT DYNAMICS, Chapter 5, John Wiley and Sons, Inc., New York, 1990.